Non-Cell Autonomous Roles for *CASK* in Optic Nerve Hypoplasia

Alicia Kerr,[1,2] Paras A. Patel,[1,2] Leslie E. W. LaConte,[1,3] Chen Liang,[1] Ching-Kang Chen,[4] Veeral Shah,[4,5] Michael A. Fox,[1,6,7] and Konark Mukherjee[1,8]

[1]Center for Neurobiology Research, Fralin Biomedical Research Institute at Virginia Tech Carilion, Roanoke, Virginia, United States
[2]Graduate Program in Translational Biology, Medicine, and Health, Virginia Tech, Blacksburg, Virginia, United States
[3]Department of Basic Science Education, Virginia Tech Carilion School of Medicine, Roanoke, Virginia, United States
[4]Department of Ophthalmology, Baylor College of Medicine, Houston, Texas, United States
[5]Texas Children's Hospital, Houston, Texas, United States
[6]Department of Biological Sciences, Virginia Tech, Blacksburg, Virginia, United States
[7]Department of Pediatrics, Virginia Tech Carilion School of Medicine, Roanoke, Virginia, United States
[8]Department of Psychiatry and Behavioral Medicine, Virginia Tech Carilion School of Medicine, Roanoke, Virginia, United States

Correspondence: Konark Mukherjee, Fralin Biomedical Research Institute at Virginia Tech Carilion, 2 Riverside Circle, Roanoke, VA 24016, USA; konark@vtc.vt.edu.
Michael A. Fox, Fralin Biomedical Research Institute at Virginia Tech Carilion, 2 Riverside Circle, Roanoke, VA 24016, USA; mafox1@vtc.vt.edu.

Submitted: March 29, 2019
Accepted: July 22, 2019

Citation: Kerr A, Patel PA, LaConte LEW, et al. Non-cell autonomous roles for *CASK* in optic nerve hypoplasia. *Invest Ophthalmol Vis Sci*. 2019;60:3584–3594. https://doi.org/10.1167/iovs.19-27197

Purpose. Heterozygous mutations in the essential X-linked gene *CASK* associate with optic nerve hypoplasia (ONH) and other retinal disorders in girls. $CASK^{+/-}$ heterozygous knockout mice with mosaic *CASK* expression exhibit ONH with a loss of retinal ganglion cells (RGCs) but no changes in retinal morphology. It remains unclear if *CASK* deficiency selectively affects RGCs or also affects other retinal cells. Furthermore, it is not known if *CASK* expression in RGCs is critical for optic nerve (ON) development and maintenance.

Methods. The visual behavior of $CASK^{+/-}$ mice was assessed and electroretinography (ERG) was performed. Using a mouse line with a floxed *CASK* gene that expresses approximately 40% *CASK* globally in all cells (hypomorph) under hemizygous and homozygous conditions, we investigated effects of *CASK* reduction on the retina and ON. *CASK* then was completely deleted from RGCs to examine its cell-autonomous role. Finally, for the first time to our knowledge, we describe a hemizygous *CASK* missense mutation in a boy with ONH.

Results. $CASK^{+/-}$ heterozygous mutant mice display reduced visual contrast sensitivity, but ERG is indistinguishable from wildtype. *CASK* hypomorph mice exhibit ONH, but deletion of *CASK* from RGCs in this background does not exacerbate the condition. The boy with ONH harbors a missense mutation (p.Pro673Leu) that destabilizes *CASK* and weakens the crucial *CASK*–neurexin interaction.

Conclusions. Our results demonstrate that mosaic or global reduction in *CASK* expression and/or function disproportionately affects RGCs. *CASK* expression in RGCs does not appear critical for cell survival, indicating a noncell autonomous role for *CASK* in the development of ON.

Keywords: optic nerve hypoplasia, *CASK*, retinal ganglion cells, non-cell autonomous

Optic nerve hypoplasia (ONH) is the most common cause of childhood blindness in developed nations, and its incidence is on the rise.[1,2] ONH involves thinning of the optic nerve (ON) and typically is associated with loss of retinal ganglion cells (RGCs) and their axons.[3] Most cases of ONH are nongenetic in nature, and therefore, the etiogenesis of ONH has remained obscure. Genetically identified forms of ONH are associated typically with transcription factors that are directly involved in the development of RGCs.[4] In many instances of ONH, however, RGCs initially begin to develop and connect with the brain, but development stalls or RGCs undergo atrophy before complete ON development.[5,6] Therefore, to better understand the etiopathogenesis of ONH, face-validated animal models of this disease must be investigated.

We demonstrated that haploinsufficiency of the X-linked gene *CASK* (calcium/calmodulin activated serine kinase) produces ONH in humans and mice.[7] Like many forms of human ONH, *CASK*-linked ONH does not affect formation of RGCs.[7] The protein product of this gene (also CASK) is a peripheral scaffolding protein,[8] and its role in RGC development or survival remains unknown. In addition to ONH, mutations in *CASK* also are associated with other retinopathies, including retinal dystrophy, indicating that retinal cells distal to RGCs also may be affected.[9–11] In previous work[7] on mice exhibiting CASK-linked ONH, we did not observe any change in lamination or loss of non-RGC retinal cells. Here, we investigated the effect of *CASK* haploinsufficiency on the function of retinal cells and determined if CASK deficiency produces an RGC-specific pathology in a cell-autonomous fashion.

Our results demonstrated that *CASK* haploinsufficiency produces isolated RGC pathology. We also demonstrated that global reduction of CASK by approximately 60% as observed in $CASK^{fl/fl}$ mice (mice with floxed *Cask* gene; stock #006382; Jackson Laboratories, Bar Harbor, ME, USA)[12] is sufficient to induce RGC loss. Surprisingly, we find that despite this

disproportionate sensitivity of RGCs to CASK deficiency, CASK expression in an RGC is not important for its survival or maintenance. Finally, using a human case report, we demonstrated that a hemizygous partial loss-of-function mutation in CASK is sufficient to produce ONH. Taken together, these results suggest that global reduction in CASK expression or function adversely affect RGC survival and CASK deficiency produces a developmental RGC pathology via a noncell autonomous mechanism.

Methods

Statement of Ethics

All experiments were performed in accordance with Virginia Tech Institutional Animal Care and Use Committee, the ARVO Statement for the Use of Animals in Ophthalmic and Vision Research, and institutional review board guidelines and approved protocols.

Visual Behavior Tasks

The two-alternative forced-swim task was performed as described previously.[13] The method is based on finding a hidden platform in response to visual cues. See Supplementary Material for full methods.

Electroretinography (ERG)

Stimulus-dependent transcorneal potential changes from both eyes were simultaneously recorded using the UTAS BigShot system (LKC Technologies, Gaithersburg, MD, USA). Photopic recordings ensued immediately after scotopic recordings by exposing the animals to a white background light of 30 Cd/m^2 intensity for 10 minutes followed by flashes of 25 Cd/s/m^2 in intensity and presented at 1 Hz frequency for 90 seconds. See Supplementary Material for full methods.

Analysis of Human *CASK* Sequence Variant

The human *CASK* sequence variant, p.Pro673Leu, was examined biochemically and in silico as described previously by us.[10,14,15] Details of the methodology are in the Supplementary Material.

Immunoblots and Immunohistochemistry (IHC)

Detailed methodology is described in the Supplementary Material. IHC was performed as described previously.[7]

In Situ Hybridization (ISH)

ISH was performed on 16-µm sections as described previously.[16,17] Sense and antisense riboprobes were generated against full-length *CASK* IMAGE Clone (catalog number MMM1013-202761641; Dharmacon, Lafayette, CO, USA). Riboprobes were synthesized using digoxigenin (DIG; Roche, Mannheim, Germany) and the MAXI-Script In Vitro Transcription Kit (Ambion, Austin, TX, USA). Probes were hydrolyzed to approximately 500 base pairs. Images were obtained on a Zeiss LSM700 confocal microscope (Carl Zeiss Meditec, Jena, Germany).

Animals

Cask$^{+/-}$ female mice generated in-house[18] were crossed with C57BL6 male mice to generate *CASK*$^{+/-}$ female pups and their *Cask*$^{+/+}$ female littermates. *Calb2-Cre* (stock #010774), *Rosa-stop-tdT* (Ai9; stock #007909), *Cask*$^{fl/fl}$ (stock #006382) all were obtained from Jackson Laboratories. Genotyping was done using a PCR-based method with primer pairs given in Supplementary Table 1. All mice used in these experiments were between 3 and 6 months old.

ON Toluidine Blue Staining and Electron Microscopy [TEM]

ON analysis was performed as described previously.[7] Details of the methodology are in the Supplementary files.

Results

Heterozygous Loss of *CASK* Produces Behavioral But Not ERG Deficits in Vision

We described previously that heterozygous loss of *Cask* (*Cask*$^{+/-}$) in mice results in ONH.[7] To assess visual function in *Cask*$^{+/-}$ mice, we used a two-alternative forced-swim task. In this task, mice learned to associate a visual cue of a sine-grating with a hidden platform used to escape the water (Fig. 1A).[19,20] Mice genetically devoid of RGCs are unable to perform this task.[13] We first assessed the ability of *Cask*$^{+/-}$ mice (and female wild-type [WT] littermates) to learn this task. *Cask*$^{+/-}$ mice and controls were trained for 8 days on a vertical grating (0.17 cycles per degree [cpd]) on the S+ monitor above a hidden platform (compared to a gray screen on the S- monitor). When their ability to locate the hidden platform in 10 trials (per day) exceeded 70%, they were considered to have successfully discriminated between the visual cues.[21] *Cask*$^{+/-}$ mice and female littermate controls performed at similar rates through the 8 days of training, and by the end of this training both genotypes were performing at near 100% accuracy (Fig. 1B).

By changing the spatial frequency of the S+ sine-grating, we were able to test visual acuity of mutant and control mice. Although *Cask*$^{+/-}$ mice performed slightly worse than littermate controls, there was no significant difference in performance regardless of the spatial frequency of the gratings (Fig. 1C). We then altered the contrast of the gratings. *Cask*$^{+/-}$ mice performed statistically worse than littermate controls in these tasks, and their performance consistently worsened (compared with littermates) as the contrast of the grating decreased (Fig. 1D). Thus, in addition to ONH and reduced RGCs, *Cask*$^{+/-}$ mice exhibited readily noticeable decreased visual performance.

To assess whether this behavioral deficit was due to ONH (and RGC loss) or from defects within the retina, ERGs were recorded on *Cask*$^{+/-}$ mice and controls. ERG waveforms are well-documented to reflect neural activity from the outer retina, with the a-wave reflecting photoreceptor activity[22] and the b-wave reflecting activity of the depolarizing bipolar cells.[23,24] Under photopic conditions, ERG b-wave responses appeared similar between *Cask*$^{+/-}$ and WT littermates (Fig. 1E). Moreover, the average photopic b-wave amplitudes elicited by light flashes of 25 Cd/sec/m^2 in intensity showed no difference between genotypes (Fig. 1F). Likewise, scotopic a-wave amplitudes also were comparable between *Cask*$^{+/-}$ and WT littermates (Figs. 1G, 1H). By fitting the ensemble scotopic b-wave amplitudes versus retinal illuminance to a modified Naka-Rushton function for maximum rod- and cone-driven responses and their half-saturating light intensities,[25] we further found their ERG responses to be very similar (Fig. 1I). Taken together, these results indicated that outer retinal function is normal in *Cask*$^{+/-}$ mice and, thus, suggested that the observed deficit in visual behavior is likely due to the loss of RGCs and their axonal thinning.

Investigative Ophthalmology & Visual Science

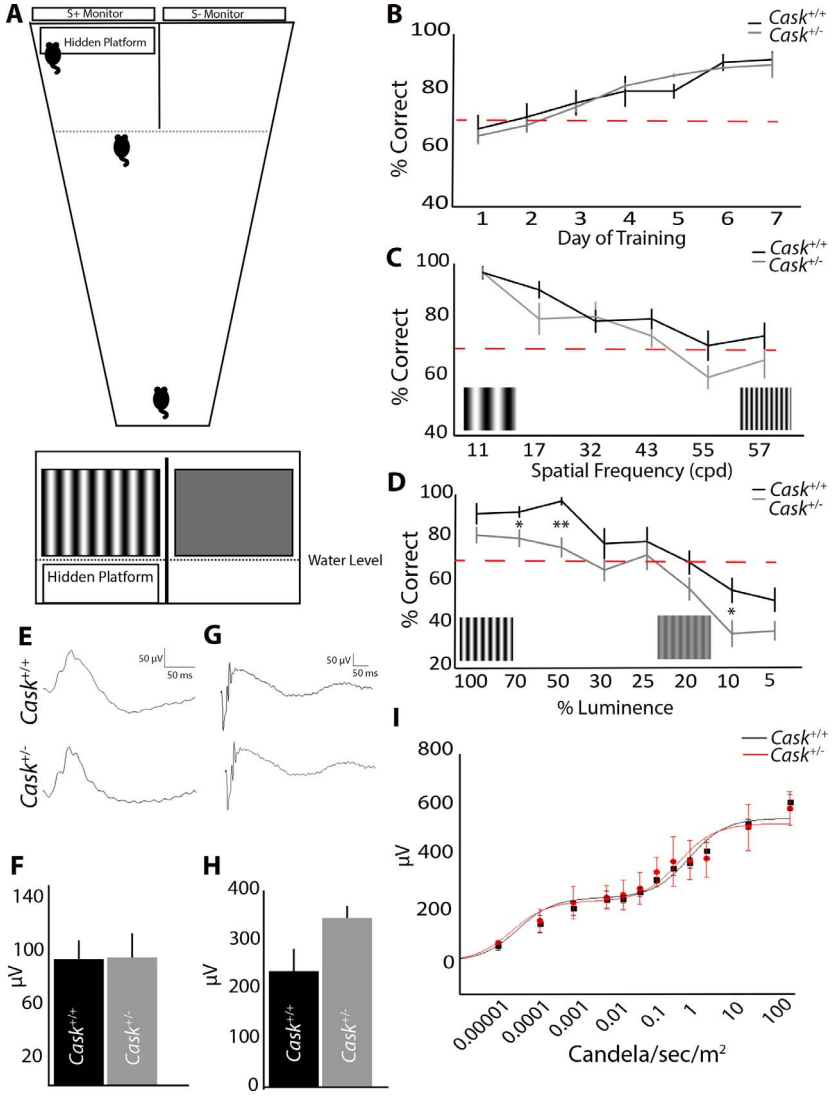

Figure 1. Heterozygous loss of *CASK* produces behavioral but not electrophysiological deficits in vision. (**A**) Schematic of two-alternative forced-swim test with a choice between a sine-positive grating (S+) and a sine-negative grating (S−). (**B**) *Cask*$^{+/-}$ and WT littermates learn the task at a similar rate. (**C**) Increasing the spatial frequency of sine-grating leads to similar decrease in *Cask*$^{+/-}$ and control mice performance. (**D**) *Cask*$^{+/-}$ mice perform significantly worse than controls when contrast (% luminance) is decreased. (**E**–**H**) Electroretinography in photopic (**E**) and scotopic conditions (**G**). $n = 3$ mice per genotype. There were no statistical differences in photopic b-wave (**F**) or scotopic a-wave (**H**) amplitudes. A Naka-Rushton fit of scotopic b-wave amplitudes versus retinal illuminance for maximum rod- and cone-driven responses reveal comparable fits between *Cask*$^{+/+}$ and *Cask*$^{+/-}$ mice (**I**). For all panels, data are plotted as mean ± SEM. $^{*}P < 0.05$, $^{**}P < 0.01$ by 2-way ANOVA.

Global Reduction in *CASK* Expression Produces ONH

Due to random X-inactivation, *CASK* heterozygous mutations result in a mosaic condition, with approximately 50% of brain cells generating 100% of *CASK* and approximately 50% of cells being CASK-null. In our experiments designed to understand the cellular role of CASK in RGCs and ON development, such mosaicism is a confounding variable. A global CASK loss-of-expression mutation, in either a hemizygous male or homozygous female mouse, is a useful model to help disentangle this confound. *Cask*$^{-/-}$ mice do not survive, but a conditional allele of *Cask* (*Cask*$^{fl/fl}$) generated previously was shown to cause a global reduction in CASK expression (~40% of WT expression) due to selection cassette interference.[12] This *Cask*$^{fl/fl}$ mouse also has been reported to have microcephaly and cerebellar hypoplasia.[18,26]

We confirmed that CASK expression in the ON of *Cask*$^{fl/fl}$ mice (Fig. 2A) is similarly reduced; therefore, we used these mice to determine if uniform reduction in *CASK* expression impacts the developing visual system. Toluidine blue sections showed that *Cask*$^{fl/fl}$ ONs are thin and hypoplastic compared to littermate *Cask*$^{+/+}$ controls (Fig. 2B), demonstrating that global reduction of CASK in all cells results in ONH.

Next, we evaluated RGC numbers in *Cask*$^{fl/fl}$, *Cask*$^{fl/+}$, and controls using a marker for RGCs (RBPMS)[27] and a Nissl stain. We saw a dose-dependent decrease in RGCs in the presence of the floxed allele of *CASK* (Fig. 2D): one floxed allele (*Cask*$^{fl/+}$) significantly reduced RGC numbers compared to controls (*Cask*$^{+/+}$), and homozygous floxed alleles (*Cask*$^{fl/fl}$) significantly reduced RGC numbers compared to heterozygotes (*Cask*$^{fl/+}$) and controls (*Cask*$^{+/+}$; Fig. 2E). This decrease is comparable to what we previously found in *Cask*$^{+/-}$ retinas (*Cask*$^{+/-}$ 27.2 ± 3.1 RBPMS^{+} cells; *Cask*$^{fl/fl}$ 30.6 ± 2.9 RBPMS^{+} cells).[7] We also evaluated total numbers of cells in the RGC layer using a

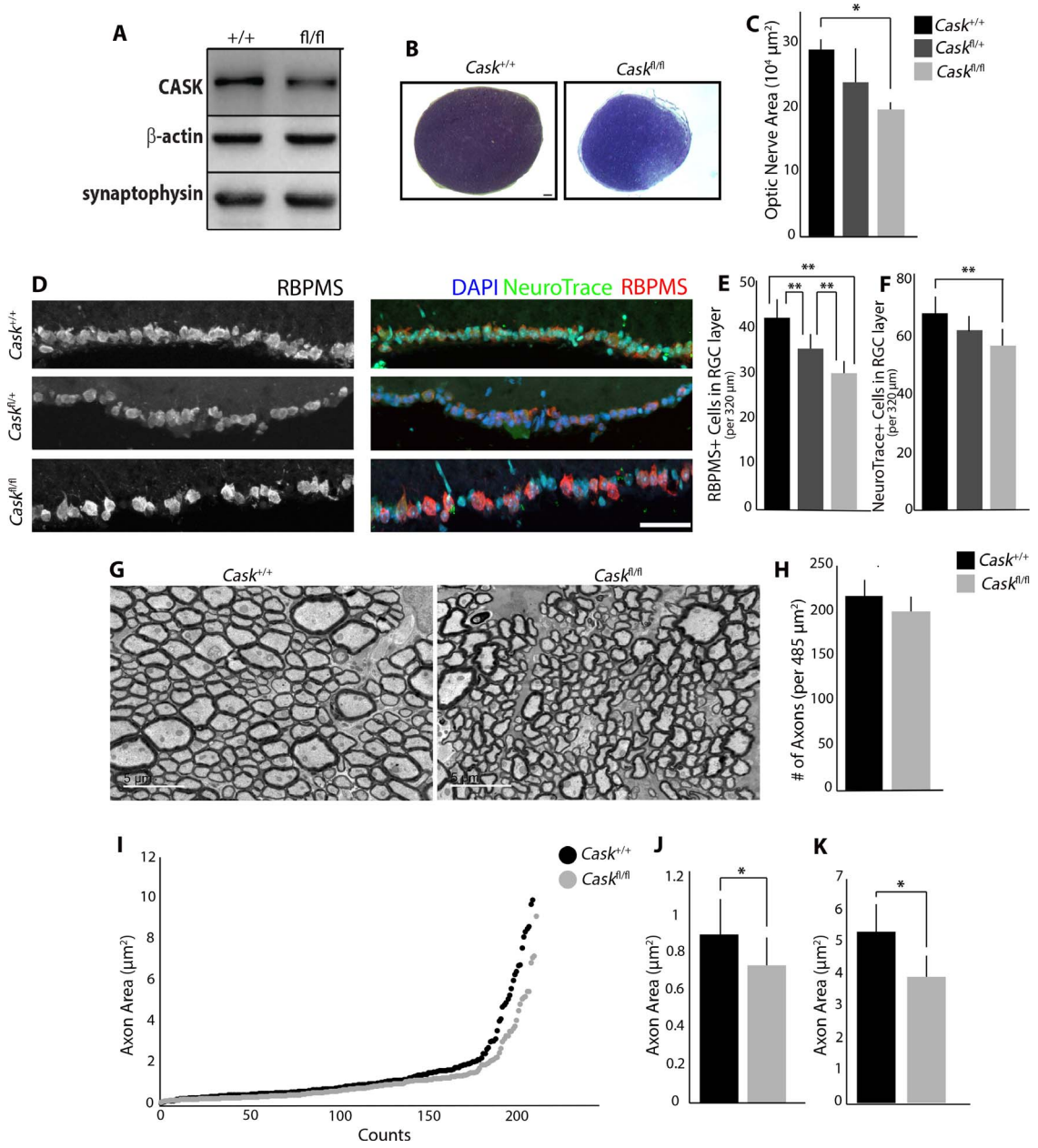

Figure 2. Global reduction in CASK expression produces ONH. (**A**) Immunoblot shows reduced levels of CASK in *Cask*$^{fl/fl}$ ON compared to WT controls. ($n = 3$ mice per genotype). (**B**) Toluidine blue staining shows reduced ON size in *Cask*$^{fl/fl}$ mice compared to WT controls. *Scale bar*: 50 μm. (**C**) Quantification of reduced cross-sectional area in *Cask*$^{fl/fl}$ compared to *Cask*$^{fl/+}$ and *Cask*$^{+/+}$ ($n = 4$ mice per genotype). (**D**) Reduction in number of cells in GCL layer using RBPMS (RNA-binding protein with multiple splicing) and NeuroTrace. *Scale bar*: 50 μm. (**E**) Quantification of reduced number of RBPMS+ cells in GCL of *Cask*$^{fl/fl}$ compared to *Cask*$^{fl/+}$ and *Cask*$^{+/+}$, and *Cask*$^{fl/+}$ compared to *Cask*$^{+/+}$ ($n = 10$ mice per genotype). (**F**) Quantification of reduced number of NeuroTrace+ cells in GCL of *Cask*$^{fl/fl}$ compared to *Cask*$^{+/+}$ ($n = 6$ mice per genotype). (**G**) TEM of RGC axons in the ON of *Cask*$^{fl/+}$ and WT controls. *Scale bar*: 5 μm. (**H**) Quantification of density of axons per image in *Cask*$^{fl/fl}$ mice ($n = 4$ mice per genotype). (**I–K**) Analysis of axon area in *Cask*$^{fl/fl}$ ON and WT controls. Quantification of the average size of fine axons (**J**) and course axons (**K**). For all panels, data are plotted as mean ± SEM; $^{*}P < 0.05$, $^{**}P < 0.01$ by 2-way ANOVA.

NeuroTrace stain to verify that RBPMS expression is not sensitive to CASK deficiency. *Cask*$^{fl/fl}$ mice have a reduction in total numbers of NeuroTrace-positive cells in the RGC layer compared to *Cask*$^{+/+}$ mice (Fig. 2F). We saw no difference in the average area of each RGC, based on measurement of RBPMS signal (WT 57.8 ± 8.6 μm^2; CASK 61.4 ± 8.7 μm^2). Finally, we explored potential axonopathy in *Cask*$^{fl/fl}$ mice. RGC axon number and diameter were evaluated using TEM of ON cross-sections from *Cask*$^{fl/fl}$ and control mice (Fig. 2G). No reduction in the density of axons in *Cask*$^{fl/fl}$ samples was observed compared to *Cask*$^{+/+}$ ONs (Fig. 2H), but we did observe a significant decrease in the average cross-sectional area of axons in *Cask*$^{fl/fl}$ ON (WT 1.54 ± 0.70 μm^2, CASK 1.20 ± 0.52 μm^2, $P < 0.05$). RGC axons in the ON can be classified as fine or coarse, based on diameter.[28,29] Previous analysis in *Cask*$^{+/-}$ mice revealed a loss of fine and coarse RGC axons.[7] When plotting RGC axon diameter, we could identify an inflection point between axon types in *Cask*$^{fl/fl}$ and controls (Fig. 2I; 2.208 μm^2 in controls). By separating the fine and coarse axons and averaging axon size for each type, we

observed that fine (Fig. 2J) and coarse axons (Fig. 2K) were significantly reduced in *Cask*$^{fl/fl}$ ON. Myelination patterns were evaluated in TEM images, and *Cask*$^{fl/fl}$ ON myelination appeared normal in adulthood. However, analysis of the ON at P12 showed a difference in total myelinated axon numbers compared to *Cask*$^{+/+}$ (Supplementary Fig. S1). This difference was no longer apparent by P18, suggesting that global reduction in *CASK* delays the onset of myelination. Overall, our data suggested RGCs are extremely sensitive to level of CASK expression.

CASK is Expressed in RGCs

To analyze the role of CASK in RGC development, we first asked if RGCs express detectable levels of CASK using in situ hybridization (Fig. 3A). Riboprobes against *Cask* mRNA were developed and revealed widespread expression in all three nuclear layers (Fig. 3B); no appreciable reactivity in these regions (versus synaptic regions) was observed with a sense riboprobe (Fig. 3C). Importantly, we observed significant reactivity of the CASK antisense riboprobe in the ganglion cell layer (GCL), suggesting CASK is generated by RGCs. Results were validated by showing CASK immunoreactivity in the GCL using IHC (Fig. 3D).

RGC-Derived *CASK* is Not Required for RGC Survival

Due to the aforementioned sensitivity of RGCs to CASK levels, we next wanted to evaluate whether RGCs were dependent upon CASK expression for survival. To remove CASK from RGCs, we sought a driver line that generated Cre recombinase in RGCs to excise the floxed *Cask* allele. One option was calretinin-Cre (*Calb2-Cre*). Calretinin is generated by RGCs, as well as some types of horizontal and amacrine cells in the developing and adult mouse retina.[30–32] Importantly, calretinin is not generated by thalamic relay cells. Furthermore, calretinin (and Cre in *Calb2-Cre* mice) is generated by RGCs at neonatal ages in mice.[13,33] The percentage of RGCs in which *Calb2-Cre* exhibited recombination activity was quantified by crossing with a reporter line (*Rosa-stop-tDT* Ai9). As expected, widespread expression of tdT was observed in the retinas of *Calb2-Cre::Rosa-stop-tdT* mice (Fig. 4A, 4A'). Cross-section analysis showed that tdT expression is present in cells of the inner nuclear layer and GCL (Fig. 4B; 77 ± 2.5% of 4′,6-diamidino-2-phenylendole (DAPI)-labeled cells in the GCL were tdT^{+}; $n = 4$ mice). Since misplaced amacrine cells also reside in the GCL and also may express Cre in this driver line (Fig. 4C), we used immunostaining for RBPMS to assess the percent of RGCs expressing Cre in this line (Fig. 4C'). We found 91.1 ± 2.4% ($n = 4$ mice) of RBPMS cells were tdT^{+} in *Calb2-Cre::Rosa-stop-tdT*. Furthermore, 87.6 ± 5.1% of the tdT^{+} cells were immunoreactive for RBPMS. It remains possible that approximately 9% of RGCs that do not generate Cre in Calb2-Cre mice belong to a small number of distinct subtypes of RGCs, such as intrinsically photosensitive RGCs (ipRGCs). This was not expected, based on scRNAseq analysis of murine RGCs, which has shown Calb2 (also known as calretinin) in all subtypes of RGCs,[34] but to address this possibility, we used IHC to show that ipRGCs and other subtypes of RGCs are labeled in Calb2-Cre mice (Supplementary Fig. S2).

To assess the requirement for CASK in RGCs, *Cask*$^{fl/fl}$::*Calb2-Cre*$^{+/+}$ mice were generated. These mutants have a global reduction in *CASK* expression (as described above), as well as a complete loss of CASK in approximately 91% of RGCs. We compared the ON of *Cask*$^{fl/fl}$::*Calb2-Cre*$^{+/+}$ mice with *Cask*$^{fl/fl}$ mice using toluidine blue staining as described earlier (Fig. 5A). Surprisingly, there was no further reduction in the size of ON when CASK was abolished from most RGCs (Fig. 5B). Furthermore, when RGCs were labeled with RBPMS and NeuroTrace (Fig. 5C), no significant loss of RGCs or overall cells in the GCL layer in the *Cask*$^{fl/fl}$::*Calb2-Cre*$^{+/+}$ mice was observed compared to *Cask*$^{fl/fl}$, suggesting that lack of *CASK* expression in remaining RGCs does not affect their survival (Figs. 5D, 5E). Finally, axonal morphology in the ON of these mutants (Fig. 5F) was assessed; there were no differences in axonal density of *Cask*$^{fl/fl}$::*Calb2-Cre*$^{+/+}$ or *Cask*$^{fl/fl}$ mice (Fig. 5G). Overall our data indicated that CASK expression in RGCs is not a requisite for RGC development or survival.

Partial Loss of Function Mutation of *CASK* in a 3-Year-Old Boy With ONH

CASK loss in males is neurodevastating and can be associated with ONH[35] and epileptic encephalopathies.[9,36] Missense mutations that decrease CASK function, however, are frequently present in males with X-linked intellectual disability who survive into adulthood. These cases typically have been reported to display nystagmus, strabismus, and even reduced visual acuity. An analysis of the optic nerve in these cases, however, has not been described. We reported a 3-year-old boy with a milder condition exhibiting microcephaly and severe pontocerebellar hypoplasia (MICPCH) similar to haploinsufficient females (Fig. 6A) and ON thinning (Fig. 6B). This subject presented with decreased visual acuity (20/130; Teller acuity test) and horizontal nystagmus (with a pendular jerk of small amplitude and frequency) that did not dampen with convergence, indicating that it may be central in origin. These phenotypes (thin ON, nonretinal defects) led to the diagnosis of ONH. Exome sequencing uncovered a *CASK* variant c.2018C>T (p.Pro673Leu) that was absent from the parents and had not been identified or reported in any other database.

We expressed recombinant CASK containing the P673L variation (CASK^{P673L}) fused with GFP protein for biochemical analysis. WT CASK (CASK^{WT}) expressed in HEK293 cells diffusely fills the cytosol (Fig. 6C), whereas expression of CASK^{P673L} results in an aggregation of protein (Fig. 6D), indicating that this protein may be partially misfolded or prone to aggregation compared to WT. CASK^{P673L} also exhibits higher insolubility, supporting the notion that this protein variant may have a propensity to misfold (Fig. 6E).

We used molecular dynamics (MD) simulations to simulate the impact of the P673L mutation on the structure of CASK. Three 100 ns MD simulation trajectories were run using a model of the CASK WT and CASK^{P673L} PDZ-SH3-GK (PSG) supradomain.[15] The radius of gyration of a protein structure model can be used to evaluate how compactly a protein structure is folded. In our simulations, CASK^{P673L}'s average radius of gyration (2.51 nm) over the course of the three trajectories is slightly, significantly larger than CASK^{WT} (2.48 nm) and the mutated structure explores a larger range of radii throughout the simulations (Supplementary Fig. S1), suggesting that the P673L mutation prevents the domain from folding as compactly and stably as it does in the WT structure. The P673L mutation also changes the overall fold of the PDZ domain more significantly (Fig. 6F) than other previously examined mutations in this domain (RMSD difference between CASK^{P673L} and WT is 3.1 nm; CASK^{M519T} RMSD difference is 2.49 nm; CASK^{G659D} RMSD difference is 2.11 nm), an important observation given *CASK*'s known interactions with proteins containing PDZ-binding domains.[37–39] A comparison of secondary structure propensity and mobility at each residue (b-factors) throughout the MD simulations helps further specify the impact of a given mutation; in the case of CASK^{P673L}, of particular interest is the notable absence in

Investigative Ophthalmology & Visual Science

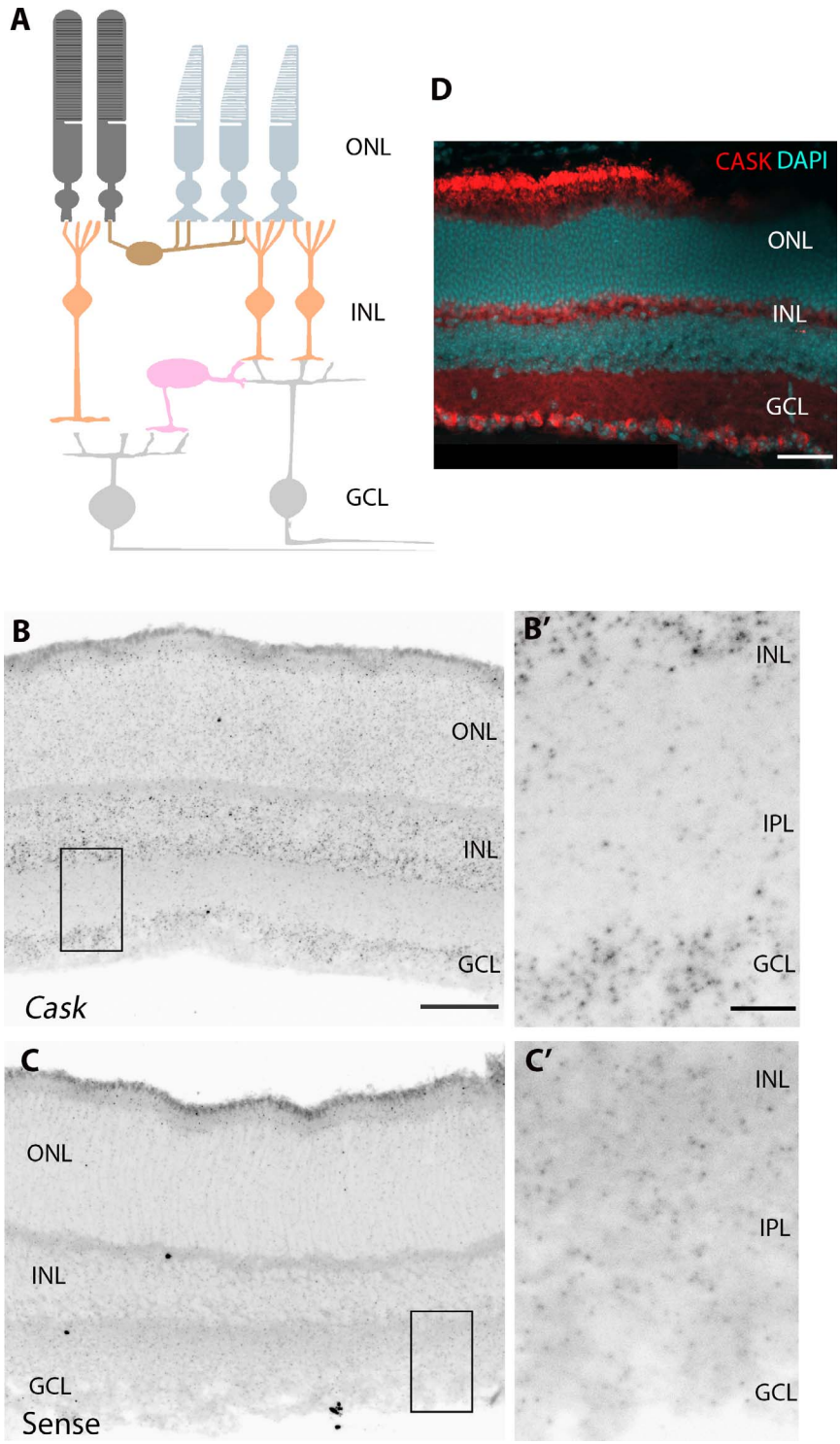

Figure 3. CASK is expressed in RGCs. (**A**) Schematic of mouse retina. ONL, outer nuclear layer; INL, inner nuclear layer; GCL, ganglion cell layer. (**B**) In situ hybridization shows *Cask* mRNA is expressed in the INL and GCL of the P14 retina. *Scale bar*: 50 µm. (**B'**) shows higher magnification of expression in GCL. *Scale bar*: 10 µm. (**C**) No appreciable signal was detected in the GCL with the sense riboprobe. (**C'**) shows higher magnification of GCL in C. (**D**) CASK immunoreactivity in the GCL of P21 retina. *Scale bar*: 50 µm.

helical propensity and mobility of the α-C helix of the CASK^{P673L} PDZ domain[40]; this particular alpha helix is purported to be involved in coupling the PDZ and SH3 domains to allow for ligand binding. The P673L variation in CASK's SH3 domain disrupts packing between all three of the domains, causing a reorientation of the domains with respect to each other (Fig. 6F). This disruption in packing may indicate that CASK^{P673L} is more likely to adopt a conformation that oligomerizes. In sum, these structural differences point to a CASK^{P673L} structure that is slightly less compact than its

Investigative Ophthalmology & Visual Science

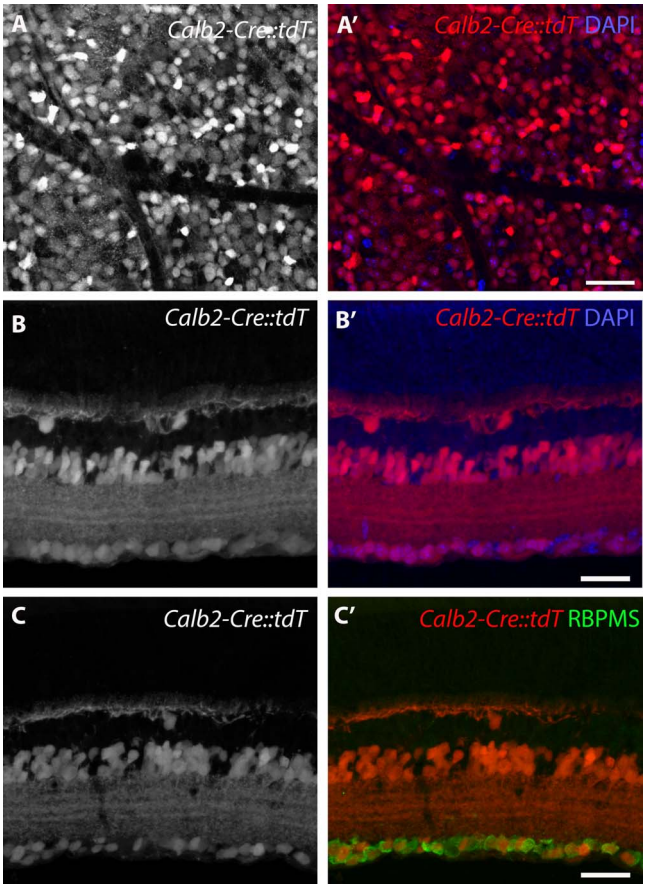

Figure 4. Calb2-Cre labels RGCs. (**A**) Retinal whole mount of the GCL of *Calb2-Cre::Rosa-stop-tdT* (*Calb2-Cre::tdT*). Note the large number of cells labeled with tdT. (**B**) Retinal cross-section of *Calb2-Cre::tdT* shows tdT^{+} cells in the INL and GCL. (**C**) tdT^{+} cells in the GCL of *Calb2-Cre::tdT* co-label with RBPMS. *Scale bar*: 50 μm, all Figures.

WT counterpart and has alterations in the region predicted to interact with known binding partners, such as neurexin.[39,41–45]

Based on the structural changes predicted by MD in $CASK^{P673L}$, we next tested these in silico predictions by determining whether the mutation indeed impairs CASK-neurexin binding in vitro by using a previously described recruitment assay where distribution of GFP-CASK can be altered from cytoplasmic to membrane-bound upon coexpression of neurexin-1β (Figs. 6C, 6G). For this recruitment assay, analysis was done only on cells where GFP-$CASK^{P673L}$ was not aggregating. Upon coexpressing neurexin-1β, $CASK^{P673L}$ and neurexin-1β did not colocalize on the membrane (Fig. 6H), revealing that neurexin is unable to efficiently recruit the remaining soluble fraction of $CASK^{P673L}$ from the cytosol. To quantitatively measure the change in $CASK^{P673L}$ affinity towards neurexin, we performed GST pulldown assays using the cytosolic tail of neurexin-1 fused to the GST protein, which revealed that the affinity of $CASK^{P673L}$ for neurexins is reduced by approximately 80% compared to $CASK^{WT}$ (Figs. 6I, 6J).

Overall, these results suggested that the P673L sequence variation affects the structure of CASK sufficiently to increase misfolding and impair but not abolish its interaction with neurexins. Such a reduction in functional CASK is sufficient to produce ONH manifestation, indicating RGCs may be highly sensitive to CASK functional deficiency. Furthermore, our data pointed to the strong possibility that other boys with CASK missense mutations also may have ONH.

Discussion

Although the prevalence of ONH is on the rise, the mechanism that underlies its onset and progression remains unknown. ONH is likely a heterogeneous disorder with differing etiologies that share similar downstream pathogenesis. Many cases of ONH arise much later in perinatal and postnatal development and are associated with environmental factors,[46,47] The mechanism of this later-onset ONH is not clear. Mouse models that target genes involved in RGC development often lead to complete nondevelopment of eyes (anophthalmy)[48] or of the ON itself[49] and, thus, do not recapitulate ONH. Heterozygous deletion of CASK produces ONH and microcephaly in girls and female mice.[7,9,18,50] We have shown that microcephaly linked to CASK mutation may stem from loss of PDZ domain-mediated interactions with proteins, like neurexin.[15] Analysis of a CASK variant ($CASK^{P673L}$) in a male subject with microcephaly and ONH suggests that microcephaly and ONH are likely to result from disruption of PDZ domain-mediated interactions of CASK. $CASK^{P673L}$'s interaction with neurexin, however, is not entirely abolished but merely reduced, indicating that this mutation causes partial loss of function in CASK. Such global CASK partial loss-of-function is compatible with survival but sufficient to produce ONH. Intriguingly, CASK mutations also have been associated with retinopathies.[9,10] These observations pose an interesting question: do CASK mutations produce isolated ONH or are the ON pathologies reflective of a broader retinal disorder? Answering this question is not only critical for more accurately classifying the ocular phenotypes seen with CASK mutations, but also is crucial for validating CASK mutant mice as tools to investigate mechanisms underlying ONH.

$Cask^{+/-}$ mice display a postnatal decrease in the number of RGCs, thinning of the ON, and atrophy of RGC axons.[7] Despite deficits in RGCs, no defects are observed in other cells or in lamination of the $Cask^{+/-}$ retina.[7] $Cask^{+/-}$ mice also exhibit significantly decreased contrast sensitivity. Based on retinal morphology and ERG data, we suggest that this visual deficit is due to RGC pathology and not due to defects in retinal circuitry. Thus, *CASK* haploinsufficiency specifically affects RGCs to produce ONH. Furthermore, we demonstrated that global reduction of CASK expression by approximately 60% also is sufficient to induce ONH, indicating that RGCs are extremely sensitive to CASK loss. Why are RGCs disproportionately affected by CASK loss? The anatomy and physiology of RGCs are unique; they are the predominant action potential-generating neurons within the retina and have extremely long, myelinated axons, unlike other retinal cells. In other brain regions, *Cask* loss or mutation appears to disproportionately affect projection neurons, such as those in pontocerebellar circuits.[9]

Since the CASK hypomorph line is based on a floxed *Cask* allele, we also used this line to delete all CASK expression from RGCs. Surprisingly, total loss of CASK from RGCs did not exacerbate the ONH phenotype, indicating RGC-derived CASK is not critical for RGC survival. How, then, does CASK reduction produce ONH? There are at least three possible explanations. First, although the discernible pathology of ONH appears late in the course of development, it is possible that the biological insult required for ONH occurs earlier in development before the Cre-mediated deletion of the CASK gene. This, however, does not explain why RGCs are more susceptible. Secondly, similar to the experimental models of glaucoma, it is possible that certain RGC subtypes[51,52] are highly susceptible to CASK deficiency and already are lost in the CASK hypomorph line; hence, no further decrease would be observed upon targeted deletion of CASK in the remaining RGCs. This would, however, suggest that the mosaic $Cask^{+/-}$

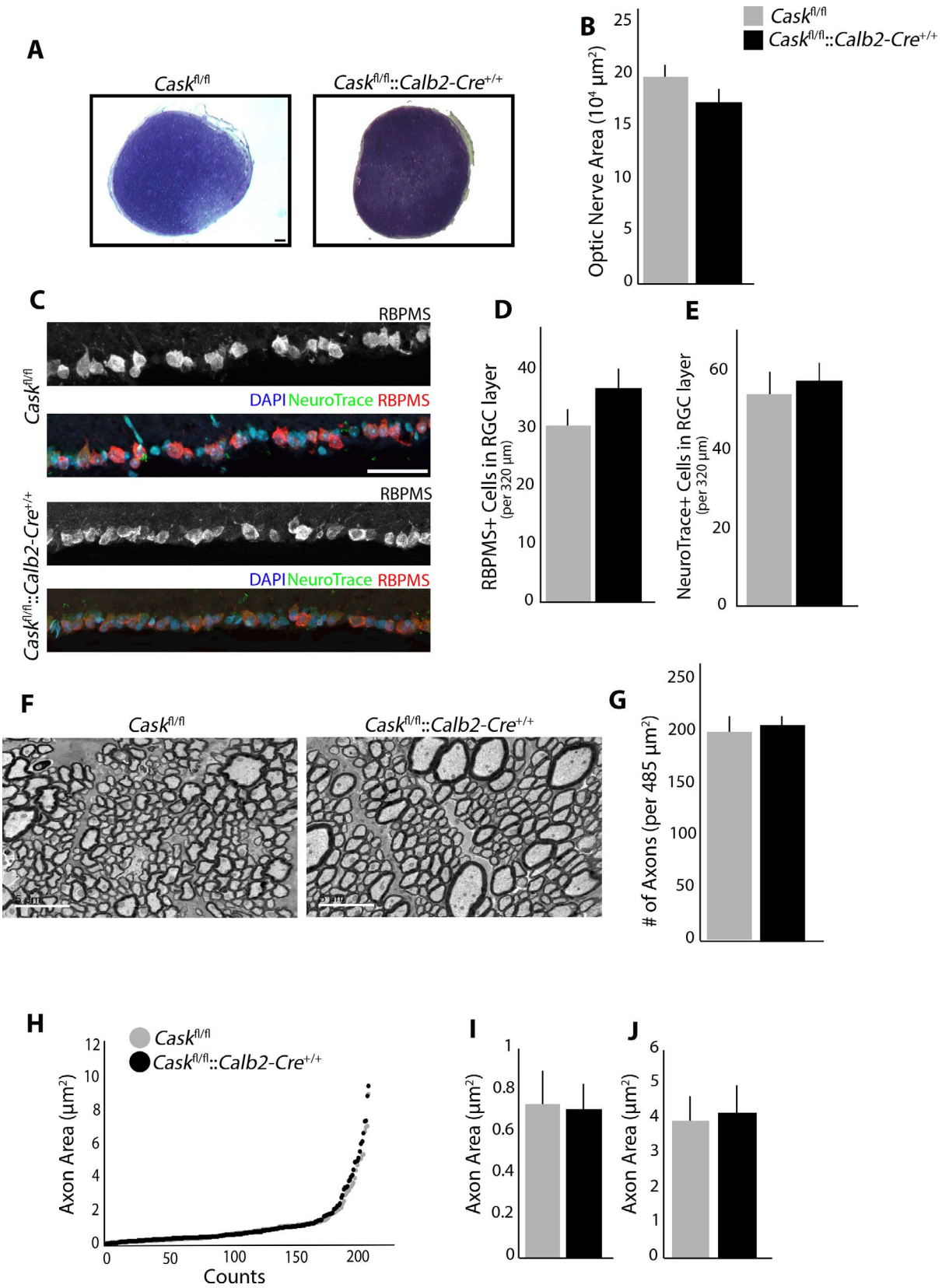

Figure 5. RGC-derived CASK is not required for RGC survival. (**A**) Toluidine blue staining shows no reduction in ON size in *Cask*$^{fl/fl}$::*Calb2-Cre*$^{+/+}$ compared to *Cask*$^{fl/fl}$. *Scale bar*: 50 µm. (**B**) Quantification of cross-sectional area in *Cask*$^{fl/fl}$::*Calb2-Cre*$^{+/+}$ compared to *Cask*$^{fl/fl}$. ($n = 4$ mice per genotype). (**C**) No reduction in number of cells in GCL layer using RBPMS (RNA-binding protein with multiple splicing) or NeuroTrace. *Scale bar*: 50 µm. (**D**) Quantification of number of cells in GCL using RBPMS in *Cask*$^{fl/fl}$::*Calb2-Cre*$^{+/+}$ compared to *Cask*$^{fl/fl}$. ($n = 10$ mice per genotype). (**E**) Quantification of number of cells in GCL using NeuroTrace in *Cask*$^{fl/fl}$::*Calb2-Cre*$^{+/+}$ compared to *Cask*$^{fl/fl}$. ($n = 6$ mice per genotype). (**F**) TEM of RGC axons in the ON in *Cask*$^{fl/fl}$::*Calb2-Cre*$^{+/+}$ compared to *Cask*$^{fl/fl}$. *Scale bar*: 5 µm. (**G**) Quantification of density of axons per image in *Cask*$^{fl/fl}$::*Calb2-Cre*$^{+/+}$ compared to *Cask*$^{fl/fl}$. ($n = 4$ mice per genotype). (**H–J**). Analysis of axon area in *Cask*$^{fl/fl}$::*Calb2-Cre*$^{+/+}$ ON compared to *Cask*$^{fl/fl}$. Quantification of the average size of fine axons (**I**) and course axons (**J**). For all panels data are plotted as mean ± SEM.

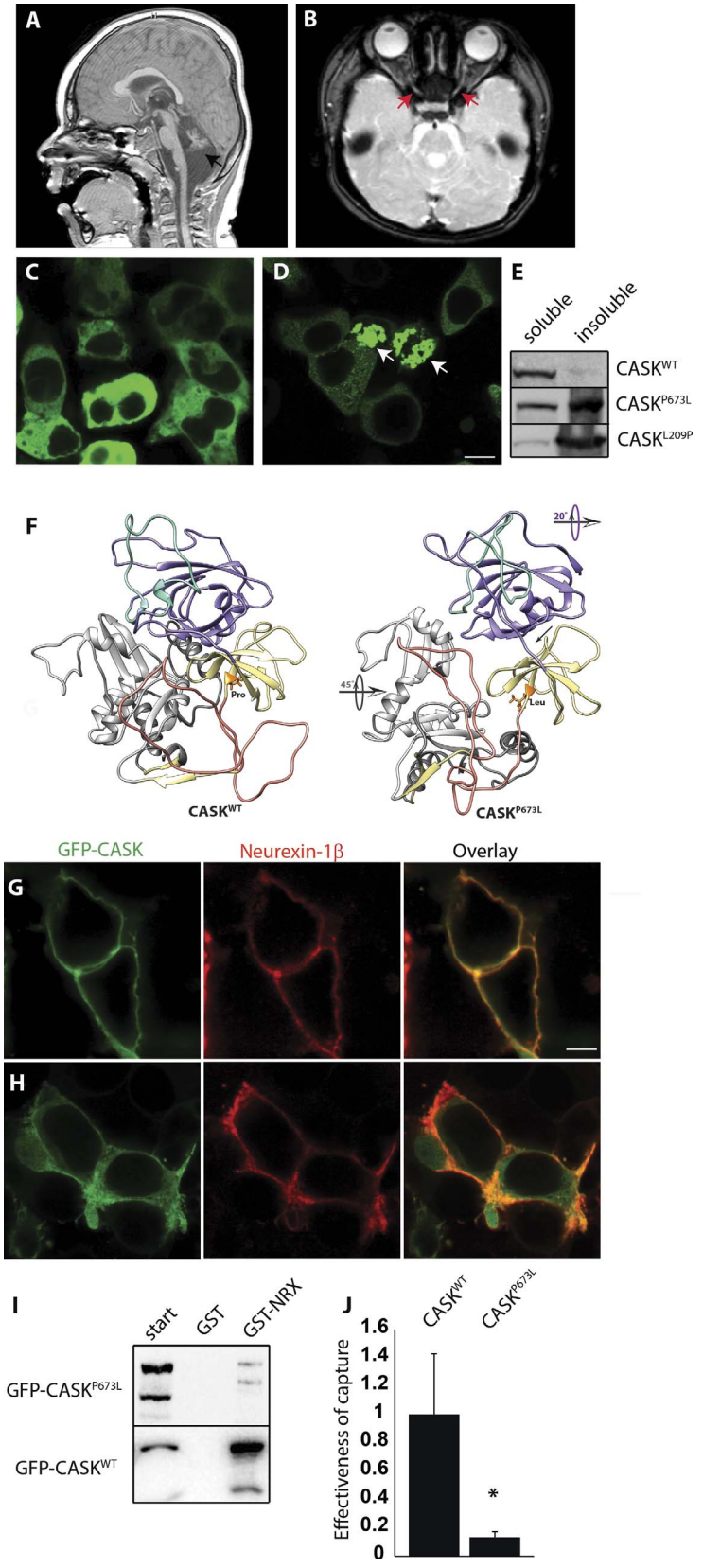

Figure 6. Partial loss of function of CASK in 3-year-old boy produces ONH. (**A**, **B**) *CASK* variant in a 3-year-old boy with microcephaly and severe pontocerebellar hypoplasia with *CASK* variant c.2018C>T (p.Pro673Leu) mutation. T2-weighted magnetic brain resonance images show small cerebellum (*black arrow*) and thinning of optic nerve (*red arrow*). (**C**) Expression of WT-CASK-GFP fusion protein in HEK293 cells shows localization of CASK in cytosol. (**D**) $CASK^{P673L}$-GFP fusion protein shows cotton-wool aggregates (*white arrows*). (**E**) Blot for CASK in soluble and soluble fractions of cell lysate show that $CASK^{P673L}$ is predominantly present in the insoluble fraction, similar to $CASK^{L209P}$, described previously to

Investigative Ophthalmology & Visual Science

have aggregation tendencies. (**F**) Structural models of the PDZ-SH3-GK supradomain of $CASK^{WT}$ (*left*) and $CASK^{P673L}$ (*right*). Site of P673L variation shown in orange, PDZ domain in *purple*, α-C helix in *green*, SH3 domain in *yellow*, hook/hinge region in *salmon*, and GK domain in *gray*. *Arrows* indicate structural differences between WT and variant structures. (**G**) Recruitment assay using a known CASK substrate, neurexin-1β, shows that $CASK^{WT}$ colocalizes with neurexin. (**H**) $CASK^{P673L}$ is mislocalized, with some colocalization with neurexin but substantial amounts visible in the cytosol. (**I**) GST-NRX is able to capture $CASK^{WT}$ but not $CASK^{P673L}$. (**J**) Effectiveness of capture for $CASK^{WT}$ and $CASK^{P673L}$ is plotted after normalization to WT. Data are plotted as mean ± SEM; $^*P < 0.05$ by 2-way ANOVA. $N = 3$. *Scale bar*: 5 μm.

mutant should have a milder phenotype than the global $Cask^{fl/fl}$ mutant, which is not the case. A third, more plausible explanation may be that the effect seen on RGCs is noncell-autonomous in origin. A strong argument for this possibility is that in $Cask^{+/-}$ mice, we do not observe secondary selection (apoptosis) of neurons resulting from random X-linked inactivation, suggesting that neurons lacking CASK do not exhibit reduced survival.[7,18] Further experiments are required in the future to fully investigate these three alternative mechanisms.

Importantly, *CASK* is present not only in neurons but also in glial and endothelial cells.[53,54] Aberrant functioning of these cell populations is likely to affect survival and health of RGCs by producing changes in retinal metabolism and vascularization. ONH has been associated with mitochondrial cytopathies,[55,56] peroxisomal disorders,[57] and nutritional deprivation,[1,58] all of which point toward a possible metabolic derangement. Similarly, altered vasculature, such as vascular tortuosity, has been suggested to be one of the hallmarks of ONH.[47,59,60] Overall our data suggested that an in-depth study of CASK mutant mice may uncover a common underlying pathobiogenesis of ONH.

Acknowledgments

The authors thank the families and children with *CASK* mutation for participation and cooperation in our studies, and Vrushali Chavan for technical help.

Supported by grants from the National Institutes of Health (NIH; Bethesda, MD, USA) Grants EY026930 and EY002520 (C-KC). Work in the Fox and Mukherjee laboratories is supported by the NIH Grants EY024712 (KM), AI124677 (MAF), and EY021222 (MAF).

Disclosure: **A. Kerr**, None; **P.A. Patel**, None; **L.E.W. LaConte**, None; **C. Liang**, None; **C.-K. Chen**, None; **V. Shah**, None; **M.A. Fox**, None; **K. Mukherjee**, None

References

1. Khaper T, Bunge M, Clark I, et al. Increasing incidence of optic nerve hypoplasia/septo-optic dysplasia spectrum: geographic clustering in Northern Canada. *Paediatr Child Health*. 2017;22:445–453.
2. Kong L, Fry M, Al-Samarraie M, Gilbert C, Steinkuller PG. An update on progress and the changing epidemiology of causes of childhood blindness worldwide. *J AAPOS*. 2012;16:501–507.
3. Katagiri S, Nishina S, Yokoi T, et al. Retinal structure and function in eyes with optic nerve hypoplasia. *Sci Repair*. 2017;7:42480.
4. Chen CA, Yin J, Lewis RA, Schaaf CP. Genetic causes of optic nerve hypoplasia. *J Med Genet*. 2017;54:441–449.
5. Frisén L, Holmegaard L. Spectrum of optic nerve hypoplasia. *Brit J Ophthalmol*. 1978;62:7–15.
6. Hoyt CS, Good WV. Do we really understand the difference between optic nerve hypoplasia and atrophy? *Eye (Lond)*. 1992;6:201–204.
7. Liang C, Kerr A, Qiu Y, et al. Optic nerve hypoplasia is a pervasive subcortical pathology of visual system in neonates. *Invest Ophthalmol Vis Sci*. 2017;58:5485–5496.
8. Butz S, Okamoto M, Sudhof TC. A tripartite protein complex with the potential to couple synaptic vesicle exocytosis to cell adhesion in brain. *Cell*. 1998;94:773–782.
9. Burglen L, Chantot-Bastaraud S, Garel C, et al. Spectrum of pontocerebellar hypoplasia in 13 girls and boys with CASK mutations: confirmation of a recognizable phenotype and first description of a male mosaic patient. *Orphanet J Rare Dis*. 2012;7:18.
10. LaConte LEW, Chavan V, DeLuca S, et al. An N-terminal heterozygous missense CASK mutation is associated with microcephaly and bilateral retinal dystrophy plus optic nerve atrophy. *Am J Med Genet A*. 2019;179:94–103.
11. Moog U, Uyanik G, Kutsche K. CASK-related disorders. In: Adam MP, Ardinger HH, Pagon RA, et al., eds. *GeneReviews*. University of Washington: Seattle, WA; 1993.
12. Atasoy D, Schoch S, Ho A, et al. Deletion of CASK in mice is lethal and impairs synaptic function. *Proc Natl Acad Sci U S A*. 2007;104:2525–2530.
13. Monavarfeshani A, Stanton G, Van Name J, et al. LRRTM1 underlies synaptic convergence in visual thalamus. *Elife*. 2018;7:e33498.
14. LaConte LE, Chavan V, Mukherjee K. Identification and glycerol-induced correction of misfolding mutations in the X-linked mental retardation gene CASK. *PLoS One*. 2014;9:e88276.
15. LaConte LEW, Chavan V, Elias AF, et al. Two microcephaly-associated novel missense mutations in CASK specifically disrupt the CASK-neurexin interaction. *Hum Genet*. 2018;137:231–246.
16. Su JM, Chen J, Lippold K, et al. Collagen-derived matricryptins promote inhibitory nerve terminal formation in the developing neocortex. *J Cell Biol*. 2016;212:721–736.
17. Su JM, Gorse K, Ramirez F, Fox MA. Collagen XIX Is Expressed by Interneurons and Contributes to the Formation of Hippocampal Synapses. *J Comp Neurol*. 2010;518:229–253.
18. Srivastava S, McMillan R, Willis J, et al. X-linked intellectual disability gene CASK regulates postnatal brain growth in a non-cell autonomous manner. *Acta Neuropathol Com*. 2016;4:30.
19. Huberman AD, Niell CM. What can mice tell us about how vision works? *Trends Neurosci*. 2011;34:464–473.
20. Prusky GT, West PWR, Douglas RM. Behavioral assessment of visual acuity in mice and rats. *Vision Res*. 2000;40:2201–2209.
21. Li S, Chen D, Sauve Y, McCandless J, Chen YJ, Chen CK. Rhodopsin-iCre transgenic mouse line for Cre-mediated rod-specific gene targeting. *Genesis*. 2005;41:73–80.
22. Brown KT. Electroretinogram - its components and their origins. *Vision Res*. 1968;8:633–677.
23. Gurevich L, Slaughter MM. Comparison of the waveforms of the ON bipolar neuron and the b-wave of the electroretinogram. *Vision Res*. 1993;33:2431–2435.
24. Stockton RA, Slaughter MM. B-wave of the electroretinogram: a reflection of on bipolar cell-activity. *J Gen Physiol*. 1989;93:101–122.
25. Tracy CM, Kolesnikov AV, Blake DR, et al. Retinal cone photoreceptors require phosducin-like protein 1 for g protein complex assembly and signaling. *PLoS One*. 2015;10:e0117129.

26. Najm J, Horn D, Wimplinger I, et al. Mutations of CASK cause an X-linked brain malformation phenotype with microcephaly and hypoplasia of the brainstem and cerebellum. *Nat Genet*. 2008;40:1065–1067.
27. Rodriguez AR, Muller LPD, Brecha NC. The RNA binding protein RBPMS is a selective marker of ganglion cells in the mammalian retina. *J Comp Neurol*. 2014;522:1411–1443.
28. Guillery R, Polley E, Torrealba F. The arrangement of axons according to fiber diameter in the optic tract of the cat. *J Neurosci*. 1982;2:714–721.
29. Williams R, Chalupa L. An analysis of axon caliber within the optic nerve of the cat: evidence of size groupings and regional organization. *J Neurosci*. 1983;3:1554–1564.
30. Nag TC, Wadhwa S. Developmental expression of calretinin immunoreactivity in the human retina and a comparison with two other EF-hand calcium-binding proteins. *Neuroscience*. 1999;91:41–50.
31. Georgi SA, Reh TA. Dicer is required for the transition from early to late progenitor state in the developing mouse retina. *J Neurosci*. 2010;30:4048–4061.
32. Bastianelli E, Takamatsu K, Okazaki K, Hidaka H, Pochet R. Hippocalcin in rat retina: comparison with Calbindin-D28k, calretinin and neurocalcin. *Exp Eye Res*. 1995;60:257–266.
33. Shi M, Zheng MH, Liu ZR, et al. DCC is specifically required for the survival of retinal ganglion and displaced amacrine cells in the developing mouse retina. *Dev Biol*. 2010;348:87–96.
34. Rheaume BA, Jereen A, Bolisetty M, et al. Single cell transcriptome profiling of retinal ganglion cells identifies cellular subtypes. *Nat Commun*. 2018;9:2759.
35. Moog U, Bierhals T, Brand K, et al. Phenotypic and molecular insights into CASK-related disorders in males. *Orphanet J Rare Dis*. 2015;10:44.
36. Saitsu H, Kato M, Osaka H, et al. CASK aberrations in male patients with Ohtahara syndrome and cerebellar hypoplasia. *Epilepsia*. 2012;53:1441–1449.
37. Fairless R, Masius H, Rohlmann A, et al. Polarized targeting of neurexins to synapses is regulated by their C-terminal sequences. *J Neurosci*. 2008;28:12969–12981.
38. Hata Y, Butz S, Sudhof TC. CASK: a novel dlg/PSD95 homolog with an N-terminal calmodulin-dependent protein kinase domain identified by interaction with neurexins. *J Neurosci*. 1996;16:2488–2494.
39. Mukherjee K, Sharma M, Urlaub H, et al. CASK Functions as a Mg2+-independent neurexin kinase. *Cell*. 2008;133:328–339.
40. Zeng ML, Ye F, Xu J, Zhang MJ. PDZ Ligand binding-induced conformational coupling of the PDZ-SH3-GK tandems in PSD-95 family MAGUKs. *J Mol Biol*. 2018;430:69–86.
41. Biederer T, Sudhof TC. CASK and protein 4.1 support F-actin nucleation on neurexins. *J Biol Chem*. 2001;276:47869–47876.
42. LaConte LEW, Chavan V, Liang C, et al. CASK stabilizes neurexin and links it to liprin-alpha in a neuronal activity-dependent manner. *Cell Mol Life Sci*. 2016;73:3599–3621.
43. Pak C, Danko T, Zhang YS, et al. Human neuropsychiatric disease modeling using conditional deletion reveals synaptic transmission defects caused by heterozygous mutations in NRXN1. *Cell Stem Cell*. 2015;17:316–328.
44. Biederer T, Sara Y, Mozhayeva M, et al. SynCAM, a synaptic adhesion molecule that drives synapse assembly. *Science*. 2002;297:1525–1531.
45. Cohen AR, Woods DF, Marfatia SM, Walther Z, Chishti AH, Anderson JM. Human CASK/LIN-2 binds syndecan-2 and protein 4.1 and localizes to the basolateral membrane of epithelial cells. *J Cell Biol*. 1998;142:129–138.
46. Hoyt CS, Billson FA. Optic-nerve hypoplasia: changing perspectives. *Aust New Zeal J Ophthalmol*. 1986;14:325–331.
47. Lambert SR, Hoyt CS, Narahara MH. Optic-nerve hypoplasia. *Surv Ophthalmol*. 1987;32:1–9.
48. Taranova OV, Magness ST, Fagan BM, et al. SOX2 is a dose-dependent regulator of retinal neural progenitor competence. *Genes Dev*. 2006;20:1187–1202.
49. Brown NL, Patel S, Brzezinski J, Glaser T. Math5 is required for retinal ganglion cell and optic nerve formation. *Development*. 2001;128:2497–2508.
50. Moog U, Kutsche K, Kortum F, et al. Phenotypic spectrum associated with CASK loss-of-function mutations. *J Med Genet*. 2011;48:741–751.
51. Daniel S, Meyer KJ, Clark AF, Anderson MG, McDowell CM. Effect of ocular hypertension on the pattern of retinal ganglion cell subtype loss in a mouse model of early-onset glaucoma. *Exp Eye Res*. 2019;185:107703.
52. Puyang Z, Chen H, Liu X. Subtype-dependent morphological and functional degeneration of retinal ganglion cells in mouse models of experimental glaucoma. *J Nat Sci*. 2015;1:e103.
53. Horng S, Therattil A, Moyon S, et al. Astrocytic tight junctions control inflammatory CNS lesion pathogenesis. *J Clin Invest*. 2017;127:3136–3151.
54. Weigand JE, Boeckel JN, Gellert P, Dimmeler S. Hypoxia-induced alternative splicing in endothelial cells. *PLoS One*. 2012;7:e42697.
55. Edvardson S, Porcelli V, Jalas C, et al. Agenesis of corpus callosum and optic nerve hypoplasia due to mutations in SLC25A1 encoding the mitochondrial citrate transporter. *J Medical Genet*. 2013;50:240–245.
56. Taban M, Cohen BH, David Rothner A, Traboulsi EI. Association of optic nerve hypoplasia with mitochondrial cytopathies. *J Child Neurol*. 2006;21:956–960.
57. Pfeifer CM, Martinot CA. Zellweger syndrome: depiction of MRI findings in early infancy at 3.0 Tesla. *Neuroradiol J*. 2017;30:442–444.
58. Garcia-Filion P, Borchert M. Prenatal determinants of optic nerve hypoplasia: review of suggested correlates and future focus. *Surv Ophthalmol*. 2013;58:610–619.
59. Cheng HC, Yen MY, Wang AG. Neuroimaging and clinical features of patients with optic nerve hypoplasia in Taiwan. *Taiwan J Ophthalmol*. 2015;5:15–18.
60. Kaur S, Jain S, Sodhi HB, Rastogi A, Kamlesh. Optic nerve hypoplasia. *Oman J Ophthalmol*. 2013;6:77–82.

Investigative Ophthalmology & Visual Science